New calculation method for initial exciton numbers on nucleon induced pre-equilibrium reactions

E. Tel,[1] A. Aydin,[2] A. Kaplan,[3] and B. Şarer[1]
[1]*Gazi University, Faculty of Arts and Sciences, Department of Physics, Ankara, Turkey*
[2]*Kirikkale University, Faculty of Arts and Sciences, Department of Physics, Kirikkale, Turkey*
[3]*Süleyman Demirel University, Faculty of Arts and Sciences, Department of Physics, Isparta, Turkey*
(Received 10 March 2008; published 23 May 2008)

In this study, we investigate the pre-equilibrium effect by using new evaluated geometry dependent hybrid model for the ^{208}Pb (p, xn) reaction at 25.5 and 62.9 MeV incident proton energies. We also suggest that the initial neutron and proton exciton numbers for the nucleon induced precompound reactions be calculated from the neutron and proton density by using an effective nucleon-nucleon interaction with Skyrme force. We calculate the initial exciton numbers obtained from SKM* and SLy4 for a proton induced reaction on target nuclei ^{208}Pb. The obtained results have been investigated and compared with the pre-equilibrium calculations and experimental results.

DOI: 10.1103/PhysRevC.77.054605 PACS number(s): 24.10.−i, 25.40.−h

I. INTRODUCTION

Pre-equilibrium processes play an important role in nuclear reactions induced by light projectiles with incident energies above about 8–10 MeV. Starting with the introduction of pre-equilibrium reactions, a series of semiclassical models of varying complexities have been developed for calculating and evaluating particle emissions in the continuum. A first model to treat intermediate process is the intranuclear cascade model (INC), where classical nucleon trajectories are followed, assuming that nucleons collide pairwise with rate and angular distributions given by the measured free nucleon-nucleon scattering results [1]. In the exciton model of Griffin [1], the partition in energy is considered that results when there is a nucleon-nucleon scattering process. A hierarch of configurations following one, two, or three, etc., nucleon-nucleon scattering events is followed, each described by the exciton number $n = p + h$, where p and h are the numbers of excited particles above the Fermi energy and below it, respectively. It was also shown that with some freedom in the choice of parameters, these models for high energy process could give reasonable fit to the observed energy and angular distributions of the emitted particles [2–4].

According to the experimental and theoretical calculation results the exciton model gave only a prescription for calculating the shape of the pre-equilibrium spectrum and the pre-equilibrium component is not described properly by the only exciton model calculations [5–8]. In this study, we have investigated the pre-equilibrium effect by using new evaluated geometry dependent hybrid model (GDH) for ^{208}Pb (p, xn) reaction. We have compared the hybrid and GDH model calculations of neutron emission spectra of ^{208}Pb (p, xn) reaction with the values reported in literature at 25.5 and 62.9 MeV incident proton energies. Besides, we have suggested that the initial neutron and proton exciton numbers for the nucleon induced precompound reactions can be calculated from the neutron and proton density by using an effective nucleon-nucleon interaction with Skyrme force. We have calculated the initial exciton numbers obtained from SKM* and SLy4 for proton induced reaction on target nuclei ^{208}Pb. The current obtained results have been also investigated and compared with the theoretical and experimental results.

II. PRECOMPOUND HYBRID AND GEOMETRY DEPENDENT HYBRID MODEL CALCULATIONS

The INC calculations results indicated that the exciton model gave only a prescription for calculating the shape of the pre-equilibrium spectrum and the exciton model deficiency resulted from a failure to properly reproduce enhanced emission from the nuclear surface [5–7]. In order to provide a first order correction for this deficiency the hybrid model was reformulated by Blann [8–10],

$$\frac{d\sigma_\upsilon(\varepsilon)}{d\varepsilon} = \sigma_R\, P_\upsilon(\varepsilon), \tag{1}$$

$$P_\upsilon(\varepsilon)d\varepsilon = \sum_{\substack{n=n_0 \\ \Delta n=+2}}^{\bar{n}} [{}_n\chi_\upsilon\, N_n(\varepsilon, U)/N_n(E)]\, g_\upsilon\, d\varepsilon \times [\lambda_c(\varepsilon)/(\lambda_c(\varepsilon) + \lambda_+(\varepsilon))]\, D_n, \tag{2}$$

where σ_R is the reaction cross section, g_υ is the single particle level density for particle type υ, ${}_n\chi_\upsilon$ is the number of particle type υ (proton or neutron) in n exciton hierarchy, $P_\upsilon(\varepsilon)d\varepsilon$ represents number of particles of the type υ emitted into the unbound continuum with channel energy between ε and $\varepsilon + d\varepsilon$. The quantity in the first set of square brackets of Eq. (2) represents the number of particles to be found (per MeV) at a given energy ε for all scattering processes leading to an "n" exciton configuration. $\lambda_c(\varepsilon)$ is emission rate of a particle into the continuum with channel energy ε and $\lambda_+(\varepsilon)$ is the intranuclear transition rate of a particle. The second set of square brackets in Eq. (2) represents the fraction of the υ type particles at a energy which should undergo emission into the continuum, rather than making an intranuclear transition. The D_n represents the average fraction of the initial population surviving to the exciton number being treated. U is the residual nucleus excitation energy, E is the composite system excitation energy ($U = E - B_\upsilon - \varepsilon$, where the B_υ is the particle binding energy), and $N_n(\varepsilon, U)$

is the number of ways. It has been demonstrated that the nucleon-nucleon scattering energy partition function $N_n(E)$ is identical to the exciton state density $\rho_n(E)$, and may be derived by the certain conditions on nucleon-nucleon scattering cross sections [11].

In the density dependent version, the GDH takes into account the density distribution of the nucleus [12]. This means a longer mean free path at the surface of the nucleus because of a lower density, and a limit to the depth of the holes below the Fermi energy. The differential emission spectrum is given in the GDH as

$$\frac{d\sigma_\upsilon(\varepsilon)}{d\varepsilon} = \pi \lambda\!\!\!^{-2} \sum_{\ell=0}^{\infty} (2\ell+1) T_\ell P_\upsilon(\ell, \varepsilon), \tag{3}$$

where $\lambda\!\!\!^{-}$ is the reduced de Broglie wavelength of the projectile and T_ℓ represents transmission coefficient for ℓth partial wave. The GDH model is made according to incoming orbital angular momentum ℓ in order to account for the effects of the nuclear-density distribution. This leads to increased emission from the surface region of the nucleus, and thus to increased emission of high-energetic particles. In this way the diffuse surface properties sampled by the higher impact parameters were crudely incorporated into the precompound decay formalism in the GDH.

The geometry dependent (surface) influences are manifested in two distinct manners in the formulation of the GDH model. The first is the longer mean free path predicted for nucleons in the diffuse surface region. It has been shown that this effect changes the predicted emission cross section about the same as would a factor of 2 increases in the mean free path in the formulation of the hybrid model, Eq. (2).

The second effect is less physically secure, yet seems to be important in reproducing experimental spectral shapes. This is the assumption that the hole depth is limited to the value of the Fermi energy which is calculated for each trajectory in a local density approximation. The result of this is to effectively reduce the degrees of freedom, especially for the higher partial waves (for which a lower maximum hole depth is predicted), thereby hardening and enhancing the predicted emission spectra. The separate influences of these two surface (geometric) effects have been illustrated by Blann [8]. In this work we assume the restriction on hole depth in the GDH model to be restricted to the first collision, for which there is some knowledge of average density at the collision site [12].

III. HARTREE-FOCK CALCULATIONS WITH SKYRME FORCE

Skyrme proposed a phenomenological nuclear force which is now called the conventional Skyrme force [13]. This force consists of some two-body terms together with a three-body term

$$V_{\rm CS} = \sum_{i<j} V_{ij}^2 + \sum_{i<j<k} V_{ijk}^3, \tag{4}$$

$$V_{ij}^2 = t_0(1+x_0 p_\sigma)\delta(\vec{r}) + \frac{1}{2} t_1 [\delta(\vec{r})\vec{k}^2 + \vec{k}'^2 \delta(\vec{r})] + t_2 \vec{k}' \delta(\vec{r}) \vec{k} + i W_0 (\vec{\sigma}_i - \vec{\sigma}_j) \bullet \vec{k} \times \delta(\vec{r}) \vec{k}, \tag{5}$$

$$V_{ijk}^3 = t_3 \delta(\vec{r}_i - \vec{r}_j) \delta(\vec{r}_j - \vec{r}_k). \tag{6}$$

The classical work of Vauthering and Brink has greatly motivated the application of the Skyrme force in the field of low energy nuclear physics [14]. They verified that, for any spin-saturated even-even nuclei, the three-body term in Eq. (4) can be replaced by a density-dependent two-body term:

$$V_{ijk}^3 \cong V_{ij}^2 = \tfrac{1}{6} t_3 \rho(\vec{R}) \delta(\vec{r}), \tag{7}$$

where $\vec{R} = \frac{1}{2}(\vec{r}_i + \vec{r}_j)$ and $\vec{r} = (\vec{r}_i - \vec{r}_j)$, the relative momentum operators $\vec{k} = \frac{\nabla_i - \nabla_j}{2i}$, acting to the right and $\vec{k}'^2 = -\frac{\nabla_i - \nabla_j}{2i}$, acting to the left [15,16]. Providing simultaneously reasonable excited state as well as ground state properties, modifications and generalizations to the conventional Skyrme force has been proposed [14–17]. Vauthering and Brink were determined two sets of conventional Skyrme force parameters (so-called SI and SIII) by fitting experimental binding energies, nucleon densities and root mean square radii [14]. Another set of modified Skyrme force, SKM based on fitting the fission barriers of heavy deformed nuclei, Brack *et al.* [16] gave a new version of SKM, which is denoted by SKM*. These Skyrme forces with the three-body term replaced by a density dependent two-body term generalized and modified, which are unified in a single form by Ge *et al.* [17] as an extended Skyrme force:

$$V_{\rm Skyrme} = \sum_{i<j} V_{ij}, \tag{8}$$

$$V_{\rm Skyrme} = t_0(1+x_0 P_\sigma)\delta(\vec{r}) + \frac{1}{2} t_1 (1+x_1 P_\sigma)\{\delta(\vec{r})\vec{k}^2 + \vec{k}'^2 \delta(\vec{r}))\} + t_2(1+x_2 P_\sigma)\vec{k}' \cdot \delta(\vec{r})\vec{k} + \frac{1}{6} t_3 (1+x_3 P_\sigma)\rho^\alpha(\vec{R})\delta(\vec{r}) + i t_4 \vec{k}' \cdot \delta(\vec{r})(\vec{\sigma}_i + \vec{\sigma}_j) \times \vec{k}, \tag{9}$$

where $\vec{k}$ is the relative momentum, $\delta(\vec{r})$ is the delta function, P_σ is the space exchange operator, $\vec{\sigma}$ is the vector of Pauli spin matrices, and $t_o, t_1, t_2, t_3, t_4, x_o, x_1, x_2, x_3, \alpha$ are Skyrme force parameters. And also the new Skyrme-like effective interactions (called Sly4) have been proposed by Chabanat *et al.* for neutron stars, supernovae and the neutron-rich nuclei [18,19]. These Sly4 parameters have been adjusted to the properties of the symmetric infinite nuclear matter, with an additional constraint on the low and high density neutron equation of state. These parameters values and the other Skyrme force parameters can be found from Refs. [14–19].

The Hartree-Fock method by using an effective interaction with Skyrme force is widely used for studying the properties of nuclei [20–24]. This method is successfully used for a wide range of nuclear characteristics such as binding energy, single particle energy, mass rms (root mean square) radii, neutron rms radii, proton rms radii, charge rms radii, charge density, neutron density, proton density, electromagnetic multiple moments, etc. The Hartree-Fock equations and pairing equations

are derived from the total energy functional of the nucleus,

$$\mathbf{E} = \mathbf{E}_{\text{Skyrme}} + \mathbf{E}_{\text{Coulomb}} + \mathbf{E}_{\text{pair}} - \mathbf{E}_{\text{c.m.}}, \tag{10}$$

where E is the total energy of the nucleus, $E_{\text{Skyrme}}$is the energy of the Skyrme interaction, $E_{\text{Coulomb}}$is the Coulomb interaction energy, $E_{\text{pair}}$is the two nucleon interaction pairing energy, and $E_{\text{c.m.}}$ is the correction for the spurious center-of-mass motion of the mean field. The densities (neutron, proton or charge)

$$\rho_q(\vec{r}) = \sum_{\beta \in q} w_\beta \psi_\beta(\vec{r})^+ \psi_\beta(\vec{r}) \quad (q : n, \text{neutron}, p, \text{proton or char, charge}), \tag{11}$$

where ψ_β is the single-particle wave function of the state β, the occupation probability of the state β is denoted by w_β.

IV. INITIAL EXCITON NUMBER CALCULATIONS FOR NUCLEON INDUCED REACTIONS

Nucleon induced reactions are assumed in the hybrid and GDH models to begin with the excitation by the projectile of a two-particle-one-hole (2p1h) doorway configuration. The incident nucleon may interact either with a nucleon of like or different isospin projection. However, in this energy range, the free scattering cross sections or interactions between nucleons of differing isospin projection is approximately three times that of nucleons of the same isospin projection. So the σ_{np} free scattering n-p cross sections are three times grater than σ_{nn} or σ_{pp}($\sigma_{np} \approx 3\sigma_{nn}$ or σ_{pp}) over the energy range of the interest for the precompound decay calculations under consideration [25].

For a neutron induced reaction on a ($N = Z$) target, one would therefore expect that there would be three n-p exciton pairs formed in the "doorway" for each $n - n$ pair. This number for other target nuclei should probably be weighted by the proton number (Z) and the neutron number (N) of the target nucleus, so that the initial number (out of two excited particles total) of neutron excitons X_n woul be given by [12]

$$X_n = \frac{2(3Z + 2N)}{(3Z + 2N + 3Z)}, \tag{12}$$

the initial proton exciton number X_p by

$$X_p = 2 - X_n, \quad X_n + X_P = 2, \tag{13}$$

The nuclear density distribution used in the hybrid model is a Fermi density distribution function,

$$\rho(R_\ell) = \rho_0[\exp(R_\ell - C)/0.55 + 1]^{-1}, \tag{14}$$

where ρ_0 is the density at the center of nucleus, and

$$C = 1.18A^{1/3}[1 - 1/(1.18A^{1/3})^2] + \lambda. \tag{15}$$

The radius for the ℓth entrance channel partial was defined by $R_\ell = \lambda(\ell + 1/2)$. In the GDH model, the Fermi energies and nuclear densities are defined to impact parameter R_ℓ [12].

The GDH model was modified by Castaneda *et al.* [26] considering neutron skin effect and they obtained the theoretical values in which better agreement with the experimental values for $^{58-64}$Ni (n, px) reaction. In order to approximate the expectation that the neutron sharp radius extends beyond the proton sharp radius. Castaneda *et al.* used Eq. (15) as the proton sharp radius, and $C + \Delta R$ for neutron sharp radius $\Delta R = 0.0235(N\text{-}Z)$, based on the droplet model result [27] for (n, px) reactions of the $^{58-64}$Ni isotopes. They suggested that the average neutron density and proton density can be calculated for entrance channel partial wave by

$$\rho(R_\ell) = \rho_0[\exp(R_\ell - C_i)/0.55 + 1]^{-1} \, (i = n, p), \tag{16}$$

where C_i for protons is C of the Eq. (15), and is $C + 0.0235(N\text{-}Z)$ for neutrons. This result is essentially equal to case of equal neutron and proton densities at low impact parameters, but gives enhanced neutron densities in the diffuse surface region. The initial neutron (n) and proton (p) exciton numbers, for each partial wave, were calculated as

$$X_n \equiv \frac{2[2\rho_n(R_l) + 3\rho_p(R_l)]}{2\rho_n(R_l) + 6\rho_p(R_l)}, \tag{17}$$

$$X_p \equiv \frac{2[3\rho_p(R_l)]}{2\rho_n(R_l) + 6\rho_p(R_l)}, \quad X_n + X_P = 2. \tag{18}$$

Equations (17) and (18) preserve the relative np/nn scattering cross section ratio of 3 used in the algorithm of Eqs. (12) and (13), but weighs collision probabilities by the nucleon densities, which have a radial dependence, rather than by the target neutron and proton numbers. It is worth reflecting qualitatively on the differences between the two methods of evaluating X_n and X_p. For a proton induced reaction on a target; the initial neutron and proton exciton numbers [6],

$$X_p = \frac{2(3N + 2Z)}{(3N + 2Z + 3N)}, \quad X_n = 2 - X_P \tag{19}$$

and for each partial wave,

$$X_p \equiv \frac{2\,[3\,\rho_n(R_l) + 2\,\rho_p(R_l)]}{3\,\rho_n(R_l) + 2\,\rho_p(R_l) + 3\,\rho_n(R_l)}. \tag{20}$$

The ALICE/ASH code is an advanced and modified version of the ALICE codes [28]. The modifications concern the implementation in the code of models describing the precompound composite particle emission, fast γ-emission, different approaches for the nuclear level density calculation, and the model for the fission fragment yield calculation. The initial exciton numbers (for protons and neutrons) in the ALICE/ASH code calculations for neutron induced reactions as

$$X_n = 2\frac{(\sigma_{np}/\sigma_{nn})Z + 2N}{2(\sigma_{np}/\sigma_{nn})Z + 2N}, \quad X_p = 2 - X_n. \tag{21}$$

The initial exciton number for proton induced reactions as

$$X_p = 2\frac{(\sigma_{pn}/\sigma_{pp})N + 2Z}{2(\sigma_{pn}/\sigma_{pp})N + 2Z}, \quad X_n = 2 - X_p, \tag{22}$$

where σ_{xy} is the nucleon-nucleon interaction cross section in the nucleus. The ratio of nucleon-nucleon cross sections calculated taking into account the Pauli principle and the nucleon motion is parameteized as

$$\sigma_{pn}/\sigma_{pp} = \sigma_{np}/\sigma_{nn} = 1.375 \times 10^{-5}T^2 - 8.734 \times 10^{-3}T + 2.776, \tag{23}$$

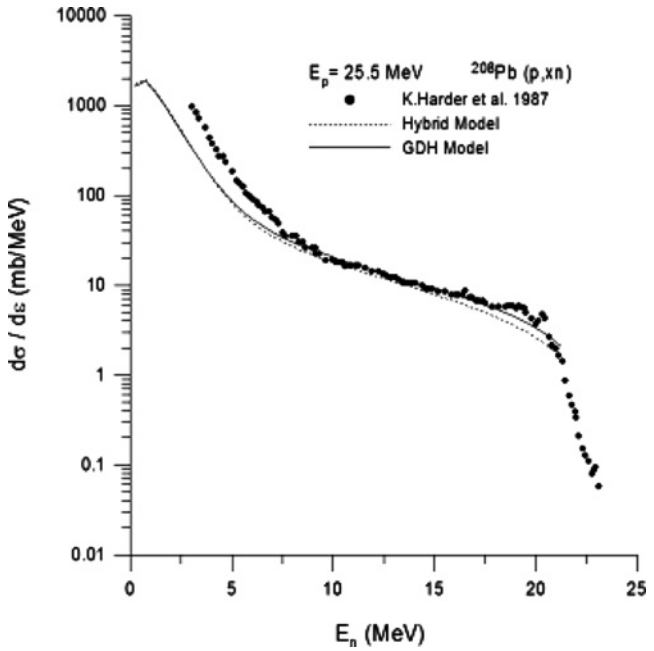

FIG. 1. The comparison of neutron emission spectra of ^{208}Pb (p, xn) reaction with the values reported in literature at 25.5 MeV incident proton energy. Experimental values were taken from Ref. [33].

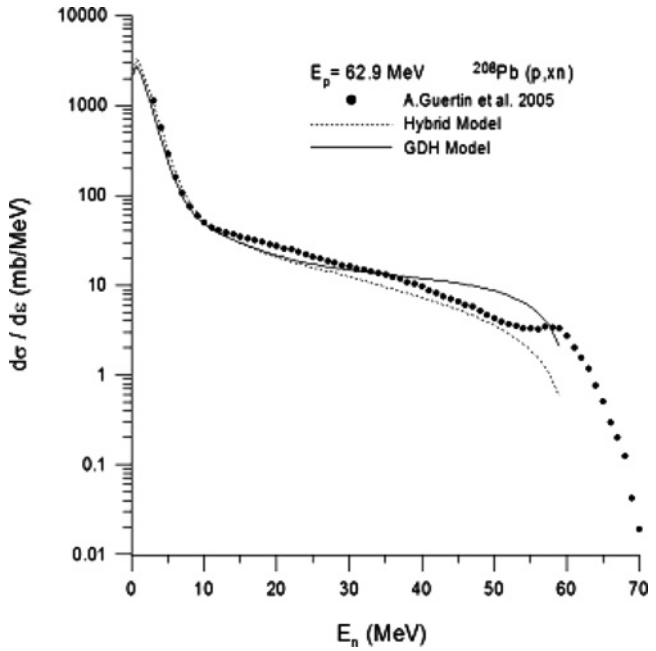

FIG. 2. The comparison of neutron emission spectra of ^{208}Pb (p, xn) reaction with the values reported in literature at 62.9 MeV incident proton energy. Experimental values were taken from Ref. [34].

where T is the kinetic energy of the projectile outside the nucleus. In details, the other all code model parameters can be found in Ref. [28].

V. RESULTS AND DISCUSSION

Recently, some new experimental data have been measured and according to these results the pre-equilibrium component is not described properly by the models included so far [29]. We have investigated the pre-equilibrium effect for the ^{208}Pb (p, xn) reaction. We have shown that comparison of the calculations of neutron emission spectra of the ^{208}Pb (p, xn) reaction with the values reported in literature at 25.5 and 62.9 MeV incident proton energies in Figs. 1 and 2. The calculations have been made in the framework of the hybrid and GDH models using the ALICE/ASH computer code. In the calculations, we used the initial exciton number $n_o = 3$ of one neutron, one proton and one hole. We used the initial exciton numbers obtained from Eqs. (22), (23) for the theoretical values of Figs. 1 and 2. By using Eqs. (22), (23), σ_{pn}/σ_{pp} values have been calculated as 2.56 and 2.28 at 25.5 and 62.9 MeV incident energies, respectively, and have been given in Table I. As can be seen that the calculated (p, xn) cross section values above about 10 MeV with GDH model have been found in better agreement with the experimental values than those of hybrid model at 25.5 MeV incident proton energy in Fig. 1. The calculated neutron emission spectra values between about 10–40 MeV with GDH model have been found in better agreement with the experimental data while the hybrid model in better agreement with the experimental values above about 40 MeV for 62.9 MeV incident proton energy in Fig. 2 (the all calculation parameters of both models have not been changed).

In the present work, we have suggested that for nucleon induced reactions cross sections, the impact parameters $\rho_n(R_l)$ and $\rho_p(R_l)$ in Eqs. (17)–(20) can be replaced with the neutron density $\rho_n(R)$and the proton density $\rho_p(R)$ from the values calculated by taking into single-particle wave functions with Eq. (11). These $\rho_n(R)$ and $\rho_p(R)$ density values can be obtained by using an effective interaction with Skyrme force.

TABLE I. The initial neutron X_n (EX1) and proton X_p (EX2) exciton numbers obtained from the ALICE/ASH code [28] and Blann and Vonach [12].

Code	$E_p = 25$ MeV			$E_p = 62.9$ MeV		
	X_n (EX1)	X_p (EX2)	σ_{pn}/σ_{pp}	X_n (EX1)	X_p (EX2)	σ_{pn}/σ_{pp}
ALICE/ASH [28]	0.80	1.20	2.56	0.78	1.22	2.28
Blann and Vonach [12]	0.82	1.18	–	0.82	1.18	–

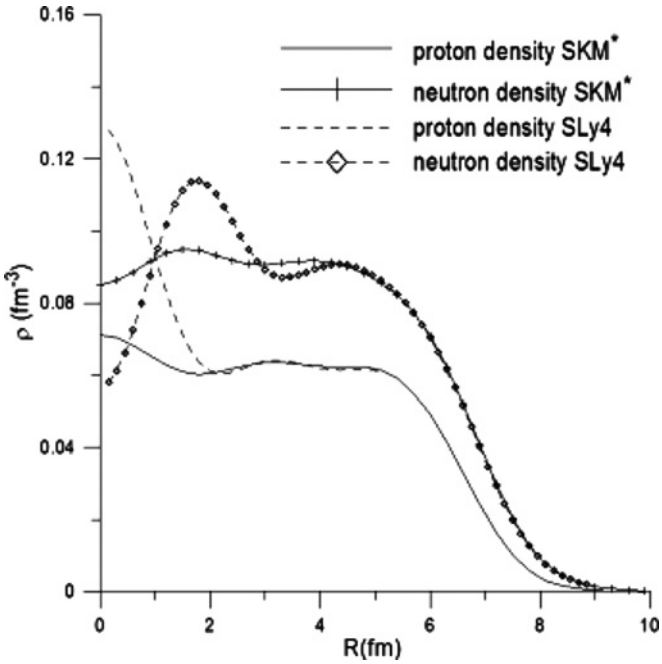

FIG. 3. Calculated neutron and proton densities of ^{208}Pb by using SKM* (with harmonic oscillator potential) and SLy4 (with Woods-Saxon potential) parameters.

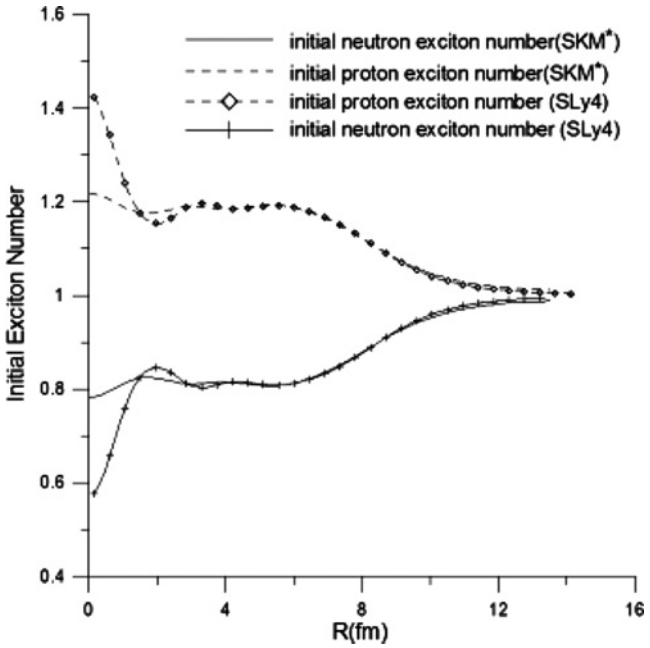

FIG. 4. Calculated density dependent the initial neutron and proton exciton numbers for proton induced reaction on target ^{208}Pb.

Therefore, for nucleon induced precompound reactions the initial neutron and proton exciton numbers can be calculated from the neutron and proton density by using an effective nucleon-nucleon interaction with Skyrme force [30].

We have calculated the neutron and proton density depending on radii by using the Hartree-Fock method with an effective interaction with Skyrme forces parameters for the ^{208}Pb target nuclei in Fig. 3. We used SKM* and SLy4 parameters for calculating the neutron and proton densities of ^{208}Pb target nuclei. The Skyrme force parameters of the SKM* and SLy4 have been given in Table II. The calculation values obtained by using SKM* parameters with the single-particle wave functions of the harmonic oscillator potential have been done with the HAFOMN code [31] and using SLy4 with the single-particle wave functions of the Woods-Saxon potential have been done with the program HARTREE-FOCK (modified for spin-orbit to accept SKI4) [32]. We have calculated the initial neutron and proton exciton numbers by using $\rho_n(R)$ and $\rho_p(R)$ density from the Eq. (19) and the obtained results have been given in Table III. We have drawn the calculated radii versus the initial exciton numbers graph obtained from SKM* and SLy4 for proton induced reaction on target nuclei ^{208}Pb in Fig. 4. The nuclear charge density distributions and charge radii provide information about the nuclear shape and the rms (root-mean-square) radii of charge distributions can be evaluated from the densities in Eq. (11):

$$r_C = \langle r_C^2 \rangle^{1/2} = \left[\frac{\int r^2 \rho_C(r) dr}{\int \rho_C(r) dr} \right]^{1/2}. \tag{24}$$

The experimental value of charge rms radii of ^{208}Pb is 5.5010 ∓ 0.0009 fm [35]. We obtained that the rms charge radii of ^{208}Pb is $r_C = 5.5127$ fm by using SKM* parameters (with harmonic oscillator wave functions) and is $r_C = 5.5065$ fm by using SLy4 parameters (with Woods-Saxon wave functions). The obtained results with new Skyrme-like (SLy4) effective interaction were found in better agreement with the experimental values.

The hybrid and GDH calculations of the ^{208}Pb (p, xn) reaction cross sections by using the different initial exciton numbers (obtained from SKM* and SLy4 parameters) were compared with the experimental values at 25.5 and 62.9 MeV incident proton energies in Figs. 5–12. The initial neutron exciton numbers have been given with EX1 (as in the same parameters of the ALICE/ASH code) and the initial proton exciton numbers with EX2 in figures. In the calculations, the all parameters of the ALICE/ASH code have been taken constant and

TABLE II. Numerical values of the parameters t_0 (MeV fm^3), t_1 (MeV fm^5), t_2 (MeV fm^5), t_3 (MeV fm$^{3\alpha}$), t_4 (MeV fm^8), w_0 (MeV fm^5), and $x_0, x_1, x_2, x_3, \alpha$ corresponding to interactions SKM* and Sly4.

Force	t_0	t_1	t_2	t_3	t_4	x_0	x_1	x_2	x_3	α	w_0
SKM*	−2645.0	410.0	−135.0	15595.0	0	0.09	0	0	0	1/6	130.0
Sly4	−2488.9	486.8	−546.4	13777.0	0	0.83	−0.34	−1	1.35	1/6	123.0

TABLE III. The calculated initial neutron X_n (EX1) and proton X_p (EX2) exciton numbers in the present work.

R (fm)	SKM*				Sly4			
	$\rho_n(R)$	$\rho_p(R)$	X_n (EX1)	X_p (EX2)	$\rho_n(R)$	$\rho_p(R)$	X_n (EX1)	X_p (EX2)
0	0.084856	0.071130	0.78	1.22	0.058062	0.128024	0.58	1.42
1.2	0.093848	0.062812	0.82	1.18	0.101920	0.083092	0.79	1.21
1.8	0.060304	0.061319	0.82	1.18	0.113993	0.063622	0.84	1.16
2.1	0.060742	0.061505	0.82	1.18	0.110255	0.060655	0.85	1.15

we have changed only the initial exciton numbers of the calculated values by using densities SKM* and SLy4 parameters.

These densities depending on the radius have been changed from the center $R = 0$ to $R = 2.1$ fm. Therefore, we have investigated the pre-equilibrium neutron emission spectra of the ^{208}Pb target nuclei for the initial exciton numbers depending on radii. The GDH calculations of the ^{208}Pb (p, xn) reaction cross sections by using the initial exciton numbers with SKM* parameters at the center ($R = 0$) have been found in good agreement with the experimental values at 25.5 MeV incident energy in Fig. 5. And also, while the calculations of emission spectra by using the initial exciton numbers with SKM* and SLy4 are distinct from each other at the center ($R = 0$), these calculations depending on increasing of radius are close to each other at center from $R = 0$ to $R = 2.1$ fm at 25.5 MeV in Figs. 5–8. In order to show this more clearly small plots which magnify the data in the 12–22 MeV energy range, were inserted into Figs. 5–8. In this way it has been seen that the GDH calculations with SKM* and Sly4 parameters by using the initial exciton numbers are closer to experimental values than the hybrid calculations at 25.5 MeV.

At 62.9 MeV incident proton energy, the results of GDH calculations with SKM* and Sly4 parameters are very close to each other for $R = 1.2$–2.1 fm and it is also possible to say that the results at hybrid calculations with the same parameters are also very close to each other at the same range of R. It can be seen the hybrid calculations with SKM* and Sly4 parameters by increasing of radius have been found in better agreement with the experimental values at 62.9 MeV in Figs. 9–12. Finally, while the GDH calculations of emission spectra by using the initial exciton numbers with SKM* and SLy4 have been found in good agreement with the experimental values at 25.5 MeV energy in Figs. 5–8, the hybrid calculations have been found in good agreement with the experimental values at 62.9 MeV in Figs. 9–12.

The nucleon induced precompound reactions for the initial neutron and proton exciton numbers can be calculated from the neutron and proton density by using an effective

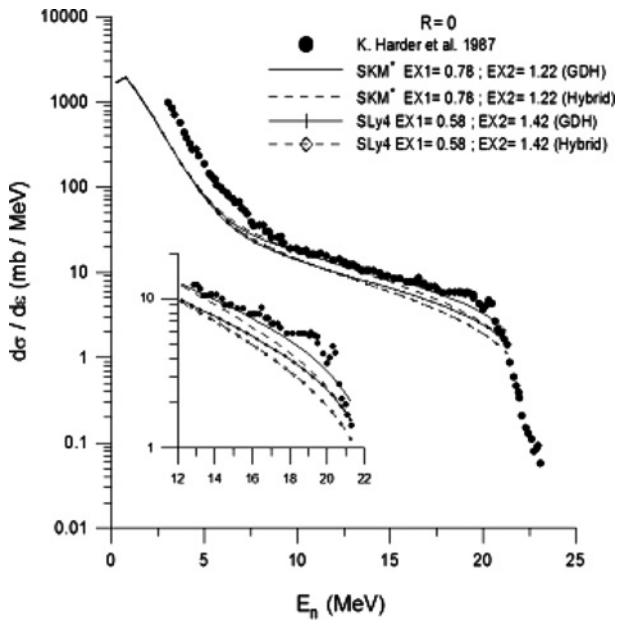

FIG. 5. The comparison of neutron emission spectra of ^{208}Pb (p, xn) reaction with the values reported in literature at 25.5 MeV proton energy. The initial exciton numbers were calculated by using neutron and proton densities at the center ($R = 0$) and experimental values were taken from Ref. [33].

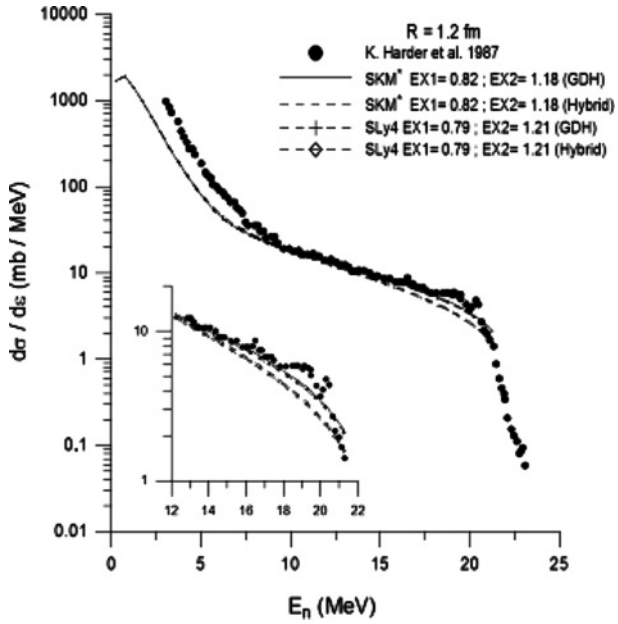

FIG. 6. The comparison of neutron emission spectra of ^{208}Pb(p, xn) reaction with the values reported in literature at 25.5 MeV proton energy. The initial exciton numbers were calculated by using neutron and proton densities at $R = 1.2$ fm and experimental values were taken from Ref. [33].

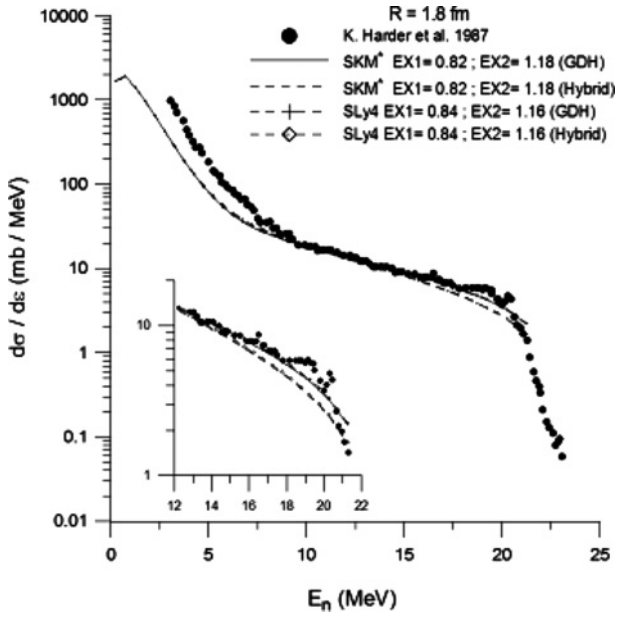

FIG. 7. The comparison of neutron emission spectra of ^{208}Pb(p, xn) reaction with the values reported in literature at 25.5 MeV proton energy. The initial exciton numbers were calculated by using neutron and proton densities at $R = 1.8$ fm and experimental values were taken from Ref. [33].

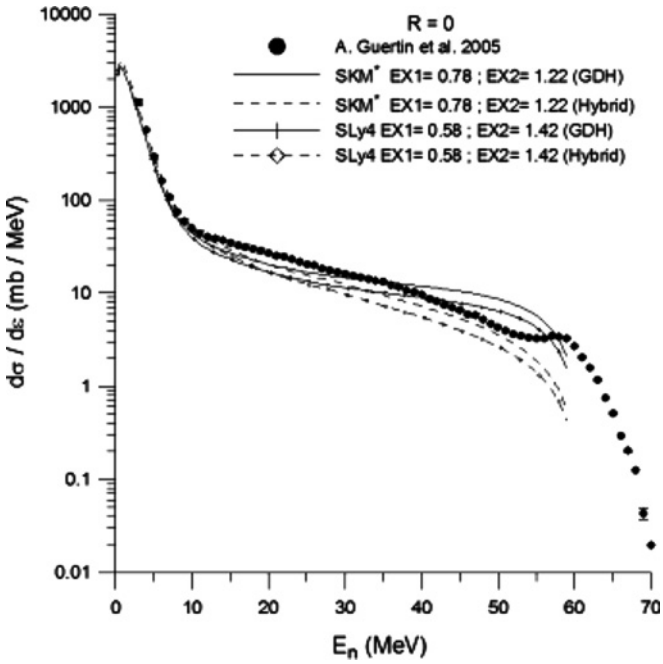

FIG. 9. The comparison of neutron emission spectra of ^{208}Pb (p, xn) reaction with the values reported in literature at 62.9 MeV proton energy. The initial exciton numbers were calculated by using neutron and proton densities at the center $(R = 0)$ and experimental values were taken from Ref. [34].

nucleon-nucleon interaction with Skyrme force. This new calculation method calculated by taking into single-particle wave functions allows an increase or decrease in precompound

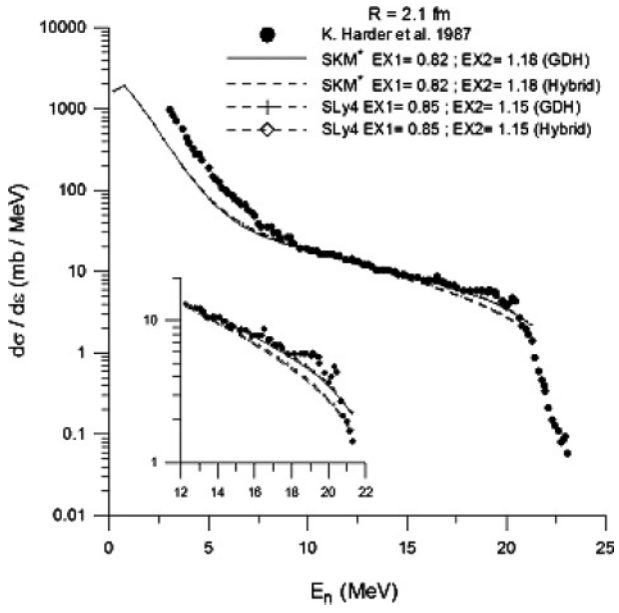

FIG. 8. The comparison of neutron emission spectra of ^{208}Pb(p, xn) reaction with the values reported in literature at 25.5 MeV proton energy. The initial exciton numbers were calculated by using neutron and proton densities at $R = 2.1$ fm and experimental values were taken from Ref. [33].

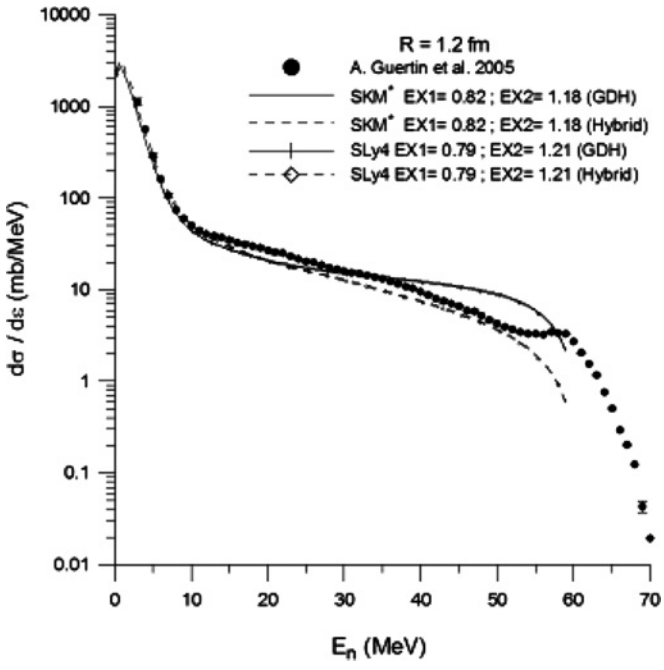

FIG. 10. The comparison of neutron emission spectra of ^{208}Pb (p, xn) reaction with the values reported in literature at 62.9 MeV proton energy. The initial exciton numbers were calculated by using neutron and proton densities at $R = 1.2$ fm and experimental values were taken from Ref. [34].

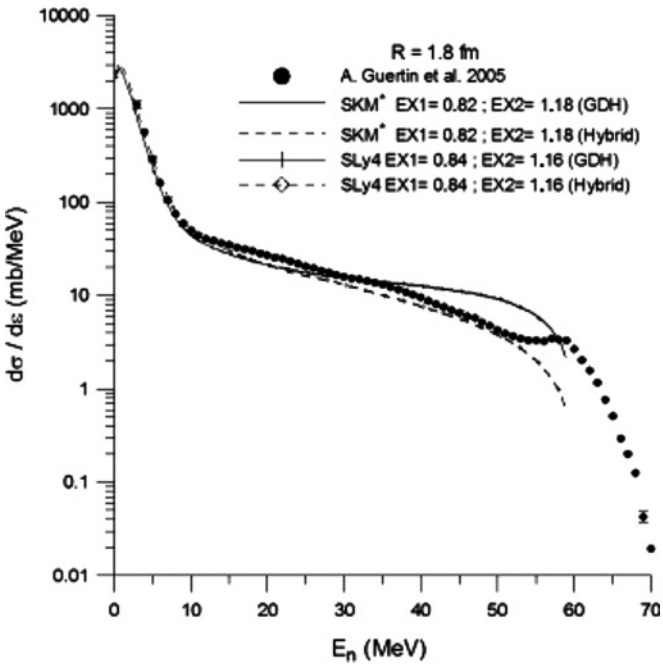

FIG. 11. The comparison of neutron emission spectra of ^{208}Pb (p, xn) reaction with the values reported in literature at 62.9 MeV proton energy. The initial exciton numbers were calculated by using neutron and proton densities at $R = 1.8$ fm and experimental values were taken from Ref. [34].

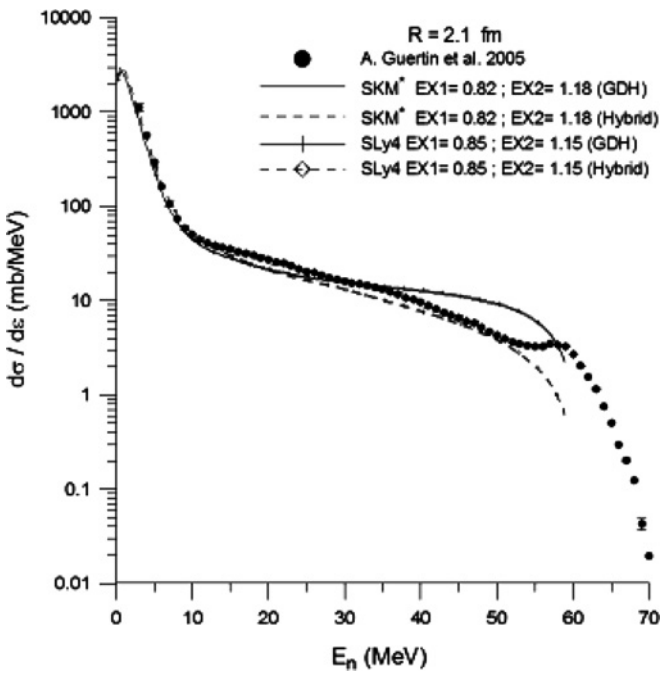

FIG. 12. The comparison of neutron emission spectra of ^{208}Pb (p, xn) reaction with the values reported in literature at 62.9 MeV proton energy. The initial exciton numbers were calculated by using neutron and proton densities at $R = 2.1$ fm and experimental values were taken from Ref. [34].

emission spectra, with simulation of effect, which are considered in the calculations, such as basic nucleon-nucleon potential interaction (such as Woods-Saxon, harmonic oscillator, etc.) for nucleon induced precompound reactions. It can be researched nuclear surface properties (and also neutron skin thickness effects) depending on the incident nucleon energy pre-equilibrium reactions and it will give more information for new nuclear reaction mechanisms researchers. Therefore, the reaction systematics can be developed and the developed reaction systematics can be used better in the estimation of unknown data and in the adoption of cross sections among discrepant experimental values.

ACKNOWLEDGMENTS

The authors wish to thank Prof. Nguyen Van Giai for the HARTREE-FOCK code with Sly4 parameters, and C. H. M. Broeders *et al*. for supporting the ALICE/ASH code and for encouragement during our present study. This work has been supported by State Planning Organization of Turkey project DPT-2006K # 120470.

[1] J. J. Griffin, Phys. Rev. Lett. **17**, 478 (1966).
[2] K. K. Gudima, S. G. Mashnik, and V. D. Toneev, Nucl. Phys. **A401**, 329 (1983).
[3] S. G. Mashnik, User Manual for the Code CEM95, Joint Institute for Nuclear Research, Dubna, Moscow Region (1995).
[4] H. Gruppelaar, P. Nagel, and P. E. Hodgson, La Rivista Del Nuovo Cimento **9**, 1 (1986).
[5] G. D. Harp and J. M. Miller, Phys. Rev. C **3**, 1847 (1971).
[6] H. Feshbach, A. Kerman, and S. Koonin, Ann. Phys. (NY) **125**, 429 (1980).
[7] T. Tamura, T. Udagawa, and H. Lenske, Phys. Rev. C **26**, 379 (1982).
[8] M. Blann, Phys. Rev. Lett. **27**, 337 (1971).
[9] M. Blann, Annu. Rev. Nucl. Sci. **25**, 123 (1975).
[10] M. Blann and J. Bisplinghoff, Livermore Lawrance Laboratory, UCID-19614 (1982).
[11] M. Blann, A. Mignerey, and W. Scobel, Nukleonika **21**, 335 (1976).
[12] M. Blann and H. K Vonach, Phys. Rev. C **28**, 1475 (1983).
[13] T. H. R. Skyrme, Phil. Mag. **1**, 1043 (1956); Nucl. Phys., **9**, 615 (1959).
[14] D. Vauthering and D. M. Brink, Phys. Rev. C **5**, 626 (1972).
[15] L. G. Qiang, J. Phys. G **17**, 1 (1991).
[16] M. Brack, C. Guet, and H. Hakasson, Phys. Rep. **123**, 275 (1986).
[17] L. X. Ge, Y. Z. Zhuo, and W. Norenberg, Nucl. Phys. **A459**, 77 (1986).
[18] E. Chabanat, P. Bonche, P. Haensel, J. Meyer, and R. Schaeffer, Phys. Scr. T **56**, 231 (1995).
[19] E. Chabanat, P. Bonche, P. Haensel, J. Meyer, and R. Schaeffer, Nucl. Phys. **A635**, 231 (1998).
[20] P. G. Reinhard and R. Y. Cusson, Nucl. Phys. **A378**, 418 (1982).
[21] P. Ring and P. Schuck, *The Nuclear Many-Body Problem* (Springer Verlag, New York, 1980).
[22] N. V. Giai and H. Sagawa, Phys. Lett. **B106**, 379 (1981).
[23] E. Tel, H. M. Şahin, A. Kaplan, A. Aydin, and T. Altınok, Ann. Nucl. Energy **35(2)**, 220 (2008).

[24] E. Tel, Ş. Okuducu, G. Tanır, N. N. Akti, and M. H. Bölükdemir, Commun. Theor. Phys. **49**, 696 (2008).
[25] K. Kikuchi and M. Kawai, *Nuclear Matter and Nuclear Reactions* (North-Holland Publishing Co., Amsterdam, 1968).
[26] C. M. Castaneda, J. L. Ullmann, F. P. Brady, J. L. Romero, N. S. P. King, and M. Blann, Phys. Rev. C **28**, 1493 (1983).
[27] W. D. Meyers, *Droplet Model of Atomic Nuclei* (IFI/Plenum, New York and London, 1977).
[28] C. H. M. Broeders, A. Yu. Konobeyev, Yu. A. Korovin, V. P. Lunev, and M. Blann, ALICE/ASH—pre-compound and evaporation model code system for calculation of excitation functions, energy and angular distributions of emitted particles in nuclear reactions at intermediate energies, FZK 7183, May 2006, http://bibliothek.fzk.de/zb/berichte/FZKA7183.pdf.
[29] E. Beták, R. Mikołajczak, J. Staniszewska, S. Mikołajewski, and E. Rurarzet, Radiochim. Acta **93(6)**, 311 (2005).
[30] E. Tel, Ph.D. thesis, Gazi University, Ankara Turkey (2000).
[31] http://www.phys.washington.edu/users/bulgac/Koonin/Skyrme_Hartree_Fock/skhafo.for
[32] P. G. Reinhard and H. Flocard, Nucl. Phys. **A584**, 467 (1995).
[33] K. Harder, A. Kaminsky, E. Mordhorst, W. Scobel, and M. Trabandt, Phys. Rev. C **36**, 834 (1987).
[34] A. Guertin, N. Marie, S. Auduc, V. Blideanu, Th. Delbar, P. Eudes, Y. Foucher, F. Haddaa, T. Kirchner, Ch. Lebrun, C. Lebrun, F. R. Lecolley, J. F. Lecolley, X. Ledoux, F. Lefebvres, T. Lefort, M. Louvel, A. Ninane, Y. Patin, Ph. Pras, G. Riviere, and C. Varignon, Eur. Phys. J. A **23**, 467 (2005).
[35] I. Angeli, At. Data Nucl. Data Tables **87**, 185 (2004).